Available online at www.sciencedirect.com
ScienceDirect
Optics Communications 267 (2006) 205–214
OPTICS COMMUNICATIONS
www.elsevier.com/locate/optcom

# Simulations of rare events in fiber optics by interacting particle systems

Josselin Garnier [a,*], Pierre Del Moral [b]

[a] Laboratoire de Probabilités et Modèles Aléatoires & Laboratoire Jacques-Louis Lions, Université Paris VII, 2 Place Jussieu, 75251 Paris Cedex 05, France
[b] Laboratoire de Mathématiques J. A. Dieudonné, Parc Valrose, 06108 Nice Cedex 2, France

Received 30 November 2005; received in revised form 11 May 2006; accepted 31 May 2006

**Abstract**

In this paper we study the robustness of linear pulses, solitons, and dispersion-managed solitons, under the influence of random perturbations. First, we address the problem of the estimation of the outage probability due to polarization-mode dispersion. Second, we compare the pulse broadening due to random fluctuations of the group-velocity dispersion. We use an original interacting particle system to estimate the tails of the probability density functions of the pulse widths. A new adaptative Monte Carlo method is applied that enforces the simulations to probe the regions of practical importance by selection and mutation steps.


*Keywords:* Polarization mode dispersion; Random dispersion; Soliton; Dispersion-managed soliton; Monte Carlo simulations

## 1. Introduction

Motivated by the growing need in massive and fast communication systems, the long-distance transmission of trains of short pulses through single-mode optical fibers has been the subject of considerable attention. The pulse candidate to be the elementary bit carrier should fulfill drastic criteria, and in particular it should be robust to various types of random perturbations, such as polarization mode dispersion (PMD) [16] or random group velocity dispersion (GVD) [25]. In modern optical telecommunication systems, it is nowadays not exceptional to require the bit-error-rate to be in the range $10^{-6}$–$10^{-12}$ [7]. As a result, the important question is not to compute the mean or the variance of the physically relevant quantity, such as the peak amplitude, the timing jitter, or the pulse width, but to estimate the tail of the probability density function (pdf) of this quantity. This issue has triggered recent work focused on the simulations of rare events in systems modeling the pulse propagation. Standard Monte Carlo (MC) simulations are usually prohibited in these situations because very few (or even zero) simulations achieve the rare event. The general approach to speeding up such simulations is to accelerate the occurrence of the rare events by using importance sampling (IS) [32]. This method has been implemented recently to deal with the timing jitter [26] and the pulse broadening induced by random GVD [27] or PMD [5,6,3]. In the IS strategy the system is simulated using a new set of input probability distributions, and unbiased estimates are recovered by multiplying the simulation output by a likelihood ratio. The tricky part in IS is to properly choose the biased distribution. The user is expected to guess a more or less correct biased distribution otherwise IS may completely fail. Recently other promising biasing MC methods have been studied, such as sampling importance resampling (SIR), sequential Monte Carlo (SMC) [10], and multicanonical Monte Carlo (MMC) [2]. In particular MMC is an iterative method that produces biased random walks that searches the state space for the important rare events. All these methods involve biasing the distributions of the input random variables to get the tail of the pdf of the output variable of interest. They are refined versions of the IS technique, in that the biased distributions are not assumed to be known a priori, but this

* Corresponding author. Tel.: +33 144278693; fax: +33 144277650.
*E-mail addresses:* garnier@math.jussieu.fr (J. Garnier), delmoral@math.unice.fr (P.D. Moral).

0030-4018/$ - see front matter © 2006 Elsevier B.V. All rights reserved.
doi:10.1016/j.optcom.2006.05.066

knowledge is accumulated during the iterations. However, these methods are *intrusive*. They require to modify the code in that the distributions of the input random variables have to be changed. Our goal is to propose a *non-intrusive* technique, that does not require to twist the input variables. The principle is to substitute for the bias of the input random variables selection steps based on the output variable. The implementation of the method has the form of an interacting particle system (IPS) with selection and mutation steps [8]. It gives an unbiased estimator of the probability of the rare event, as well as an estimator of the error variance. The interacting particle methodology is closely related to a class of Monte Carlo acceptance/rejection simulation techniques used in physics and biology. These methods were first designed in the fifties to estimate particle energy transmission [19], self-avoiding random walks, and macromolecule evolutions [31]. The present paper is devoted to new applications towards rare event estimation in optical telecommunications.

Our goal is twofold. First, we address two important practical problems and we clarify the behaviors of the pdf tails of the pulse widths induced by random GVD and PMD. Second, we show that the IPS strategy can be used to reduce the computational costs of generating pdf tails in different configurations and regimes, and thus it is most likely that it could be applied in other situations. As we point out in the paper, the major advantage of the IPS method compared to IS and MMC is that it is non-intrusive and it does not require to simulate the system with a biased distribution.

## 2. The interacting particle system

Let us consider a physical quantity $X$ whose evolution can be described by the random recursive equation

$$X_{k+1} = \Phi(X_k, ,\theta_k), \tag{1}$$

where $(\theta_k)_{k\geqslant 0}$ is a sequence of independent random variables and $\Phi$ is a known function. A practical situation addressed in this paper is the propagation of a pulse in a randomly perturbed optical fiber. In this case, $X_k$ is the pulse profile at the output of the $k$th (fictitious) fiber segment, $\theta_k$ describes the random perturbations of the $k$th fiber segment (say, the spatial GVD fluctuations), and $\Phi(X,\theta)$ is the output pulse profile driven by the perturbation $\theta$ when the input pulse profile is $X$. We may think that the output profile is computed by a non-linear Schrödinger equation with random coefficients described by $\theta$. The problem consists in estimating the tail of the pdf of the random quantity $V(X_n)$ where $V$ is a real-valued function and $n$ corresponds to a given final "time" $n$. In our example, the "time" corresponds to the label of a fiber segment and $V(X)$ is the width of the pulse profile $X$ (it could be also the peak power, or any scalar characteristic parameter of the profile $X$).

The IPS consists of a set of $N$ particles $(X_k^{(i)})_{1\leqslant i\leqslant N}$ evolving from "time" $k=0$ to $k=n$. The initial generation at $p=0$ is a set of copies of $X_0$. The updating from the generation $k$ to the generation $k+1$ is divided into two stages.

(1) The selection stage

$$(X_k^{(i)})_{1\leqslant i\leqslant N} \mapsto (\check{X}_k^{(i)})_{1\leqslant i\leqslant N}$$

consists in choosing randomly and independently $N$ particles amongst $(X_k^{(i)})_{1\leqslant i\leqslant N}$ as follows. For each $j=1,\ldots,N$, $\check{X}_k^{(j)}$ can take one of the $N$ values $(X_k^{(i)})_{1\leqslant i\leqslant N}$ with probability

$$\mathbb{P}\left(\check{X} = X_k^{(i)}\right) = \frac{G_k(X_k^{(i)})}{\sum_{l=1}^{N} G_k(X_k^{(l)})}$$

for $i=1,\ldots,N$. We discuss below the choice of the weight function $G_k$ (that depends on $V$). Roughly speaking, $G_k$ is increasing with $V$, so that particles with low scores $V(X_k^{(i)})$ are likely to be killed, while particles with high scores are multiplied. Note that the total number of particles is kept constant.

(2) The mutation step

$$(\check{X}_k^{(i)})_{1\leqslant i\leqslant N} \mapsto (X_{k+1}^{(i)})_{1\leqslant i\leqslant N}$$

consists in mutating independently the particles according to the recursive equation (1):

$$X_{k+1}^{(i)} = \Phi(\check{X}_k^{(i)}, \theta_k^{(i)}),$$

where $(\theta_k^{(i)})_{1\leqslant i\leqslant N}$ are independent copies of $\theta_k$. Note that the true distribution of $\theta_k$ is applied, in contrast with IS.

The description is rough in that the IPS actually acts on the path level. The mathematical tricky part consists in proposing an unbiased estimator of the pdf tail and analyzing its variance. The variance analysis provides useful information for a proper choice of the weight function of the selection stage.

We now report the general results presented in an abstract framework in Ref. [9] and we apply them to propose an efficient estimator of the pdf tail of $V(X_n)$. The quality of the estimator depends on the choice on the weight function $G_k$ that controls the selection stage of the IPS. We have examined in Ref. [9] different weight functions and a thorough analysis has proved that quasi-optimal results can be obtained with the weight function

$$G_k(X) = \exp[\alpha(V(X_k) - V(X_{k-1}))] \tag{2}$$

parameterized by $\alpha > 0$. In particular we have shown that weight functions of the type $G_k(X) = \exp[\beta V(X_k)]$ were less efficient in the sense that the variances of the estimators were larger. This is a manifestation of one of the most surprising conclusions obtained in Ref. [9]: it is not efficient to select the "best" particles at each generation (i.e. those with the highest values $V(X_k)$), but it is much more efficient to select amongst the particles with the best increments (i.e. those with the highest values of $V(X_k) - V(X_{k-1})$).

The practical implementation of the IPS is as follows.

*Initialization*

We start with a set of $N$ identical initial conditions $\widehat{X}_0^{(i)} = X_0$, $1 \leqslant i \leqslant N$. This set is complemented with a set of weights $\widehat{W}_0^{(i)} = 0$, $1 \leqslant i \leqslant N$. This forms a set of $N$ particles: $(\widehat{W}_0^{(i)}, \widehat{X}_0^{(i)})$, $1 \leqslant i \leqslant N$, where a particle is a pair $(\widehat{W}, \widehat{X})$ with $\widehat{W} \in \mathbb{R}^+$.

Now, assume that we have a set of $N$ particles at time $k$ denoted by $(\widehat{W}_k^{(i)}, \widehat{X}_k^{(i)})$, $1 \leqslant i \leqslant N$.

*Selection*

We first compute the normalizing constant

$$\hat{\eta}_k^N = \frac{1}{N} \sum_{i=1}^{N} \exp[\alpha(V(\widehat{X}_k^{(i)}) - \widehat{W}_k^{(i)})]. \tag{3}$$

We choose independently $N$ particles according to the Boltzmann–Gibbs distribution for $1 \leqslant i \leqslant N$,

$$\mathbb{P}\left((\check{W}, \check{X}) = (\widehat{W}_k^{(i)}, \widehat{X}_k^{(i)})\right) = \frac{1}{N\hat{\eta}_p^N} \exp\left[\alpha\left(V(\widehat{X}_k^{(i)}) - \widehat{W}_k^{(i)}\right)\right].$$

This means that particles with low scores are killed, while particles with high scores are multiplied. The new particles are denoted by $(\check{W}_k^{(i)}, \check{X}_k^{(i)})$, $1 \leqslant i \leqslant N$.

*Mutation*

For every $1 \leqslant i \leqslant N$, the particle $(\check{W}_k^{(i)}, \check{X}_k^{(i)})$ is transformed into $(\widehat{W}_{k+1}^{(i)}, \widehat{X}_{k+1}^{(i)})$ by the recursive equation $\widehat{X}_{k+1}^{(i)} = \Phi(\check{X}_k^{(i)}, \theta_k^{(i)})$ where the perturbations $\theta_k^{(i)}$ are independent copies of the random variable $\theta_k$. Finally we set $\widehat{W}_{k+1}^{(i)} = V(\check{X}_k^{(i)})$.

Let us now focus our attention to the estimation of the pdf tail of $V(X_n)$. We use the estimator $p^N(a) = (\delta a)^{-1} P^N_{[a,a+\delta a)}$ with a small $\delta a$, where

$$P^N_{[a,a+\delta a)} = \left[\frac{1}{N} \sum_{i=1}^{N} \mathbf{1}_{[a,a+\delta a)}(V(\widehat{X}_n^{(i)})) \exp\left(-\alpha \widehat{W}_n^{(i)}\right)\right] \times \left[\prod_{k=0}^{n-1} \hat{\eta}_k^N\right]. \tag{4}$$

As shown in Ref. [9] this estimator is unbiased in the sense that

$$\mathbb{E}[P^N_{[a,a+\delta a)}] = \mathbb{P}(V(X_n) \in [a, a+\delta a)),$$

where $\mathbb{E}$ stands for the expectation with respect to the distribution of the $(\theta_k)_{0 \leqslant k \leqslant n-1}$. The central limit theorem for the pdf estimator takes the form

$$\sqrt{N}(p^N(a) - p(a)) \overset{N\to\infty}{\to} \mathcal{N}(0, p_2^2(a)),$$

where $\mathcal{N}(0, p_2^2(a))$ is a zero-mean Gaussian random variable with variance $p_2^2(a)$. The variance $p_2^2(a)$ can be estimated by $(\delta a)^{-1} Q^N_{[a,a+\delta a)}$, where

$$Q^N_{[a,a+\delta a)} = \left[\frac{1}{N} \sum_{i=1}^{N} \mathbf{1}_{[a,a+\delta a)}\left(V\left(\widehat{X}_n^{(i)}\right)\right) \exp\left(-2\alpha \widehat{W}_n^{(i)}\right)\right] \times \left[\prod_{k=0}^{n-1} \hat{\eta}_k^N\right]^2. \tag{5}$$

The estimator of the variance is important because confidence intervals can then be obtained. Performance comparisons based on the evaluation of the variance $p_2^2(a)$ were proposed in Ref. [9] between standard MC, IS and IPS. These comparisons were carried out theoretically in an abstract framework, and practically on a toy model where explicit but long computations were possible. The conclusions were that IS with an appropriate biased distribution and IPS with a suitable selection pressure function (2) had similar error variances, in the sense that $p_2(a) \sim p(a)$ in both cases. This shows a dramatic performance improvement compared with standard MC, where $p_2(a) \sim p(a)^{1/2}$. In fact, IPS performance is slightly below IS, because of a multiplicative factor of the order of $\sqrt{n}$ for $p_2(a)$, where $n$ is the number of generations, of the order of 10–100. This shows that IPS cannot perform better than IS if an efficient biased distribution is known a priori and can be implemented. However, our main goal is precisely to propose a non-intrusive method that does not require such an implementation. Note also that the theoretical analysis shows that the IPS method is efficient in the limit of a large number of particles. A priori, it is not easy to predict the minimal number of particles that ensure a robust estimation. However, a posteriori, the estimator (5) of the variance can be used to check the accuracy of the prediction. We shall illustrate this assertion in the next two sections, where we apply the IPS strategy to compute the probabilities of rare events in problems relevant to fiber optics.

## 3. Polarization mode dispersion in optical fibers

### 3.1. Introduction

The study of pulse propagation in a fiber with random birefringence has become of great interest for telecommunication applications. Recent experiments have shown that polarization mode dispersion (PMD) is one of the main limitations on fiber transmission links because it can involve significant pulse broadening [16]. PMD has its origin in the birefringence [37], i.e. the fact that the electric field is a vector field and the index of refraction of the medium depends on the polarization state (i.e. the unit vector pointing in the direction of the electric vector field). Random birefringence results from variations of the fiber parameters such as the core radius or geometry. There exist various physical reasons for the fluctuations of the fiber parameters. They may be induced by mechanical distortions on fibers in practical use, such as point-like pressures or twists [30]. They may also result from variations of ambient temperature or other environmental parameters [5].

The difficulty is that PMD is a random phenomenon. Designers want to ensure that some exceptional but very annoying event occurs only a very small fraction of time. This critical event corresponds to a pulse spreading beyond a threshold value. For example, a designer might require

that such an event occurs less than 1 min per year [7]. PMD in an optical fiber varies with time due to vibrations and variations of environmental parameters. The usual assumption is that the fiber passes ergodically through all possible realizations. Accordingly requiring that an event occurs a fraction of time $p$ is equivalent to require that the probability of this event is $p$. The problem is then reduced to the estimation of the probability of a rare event. Typically the probability is $10^{-6}$ or less [7]. It is extremely difficult to use either laboratory experiments or MC simulations to obtain a reliable estimate of such a low probability because the number of configurations that must be explored is very large. Recently IS has been applied to numerical simulations of PMD [5]. This method gives good results, however it requires very good physical insight into the problem because it is necessary for the user to know how to produce artificially large pulse widths. We would like to revisit this work by applying the IPS strategy. The main advantage is that we do not need to specify how to produce artificially large pulse widths, as the IPS will automatically select the good "particles".

### 3.2. Review of PMD models

The pulse spreading in a randomly birefringent fiber is characterized by the so-called differential group delay (DGD) $\tau = |\hat{\mathbf{r}}|$ which is a function of the propagation distance $z$ and frequency $\omega$. The three-dimensional vector $\hat{\mathbf{r}}$ is the so-called PMD vector, which is solution of

$$\hat{\mathbf{r}}_z = \omega\Omega(z) \times \hat{\mathbf{r}} + \Omega(z), \tag{6}$$

where $\Omega(z)$ is a three-dimensional zero-mean stationary random process modeling PMD. Simplified analytical models have been studied. In the standard model [29,37,16] it is assumed that the process $\Omega$ is a white noise with autocorrelation function $\mathbb{E}[\Omega_i(z')\Omega_j(z)] = \sigma^2\delta_{ij}\delta(z'-z)$, $1 \leqslant i,j \leqslant 3$. It is then easy to establish [15] that the DGD $\tau$ is a diffusion process. If $\hat{\mathbf{r}}(0) = (0,0,0)^{\mathrm{T}}$, then $\tau(z)$ obeys a Maxwellian distribution with pdf

$$p(\tau) = \frac{\sqrt{2}\tau^2}{\sqrt{\pi}(\sigma^2 z)^{3/2}} \exp\left(-\frac{\tau^2}{2\sigma^2 z}\right)\mathbf{1}_{[0,\infty)}(\tau).$$

The white noise model gives an analytical formula for the pdf of the DGD, which in turns allows us to compute exactly the probability that the DGD exceeds a given threshold value. However it has been pointed out that the pdf tail of the DGD does not fit with the Maxwellian distribution in realistic configurations [4]. Various numerical and experimental PMD generation techniques involve the concatenation of birefringent elements with piecewise constant vectors $\Omega$ [24]. Eq. (6) can be solved over each segment, and continuity conditions on the segments junctions give a discrete model for the PMD vector $\hat{\mathbf{r}}$. The total PMD vector at the output of the $k$th section can then be obtained from the concatenation equation [17]

$$\hat{\mathbf{r}}_{k+1} = R_k\hat{\mathbf{r}}_k + \sigma\Omega_k, \tag{7}$$

where $\sigma$ is the DGD per section. Assuming linearly birefringent fibers, $\Omega_k$ lies in the equatorial plane of the Poincaré sphere [13]: $\Omega_k = \Omega(\psi_k)$ with

$$\Omega(\psi) = (\cos(\psi), \sin(\psi), 0)^{\mathrm{T}}.$$

$R_k$ is a matrix corresponding to a rotation through an angle $\phi_k$ about the axis $\Omega_k$ [17]. Explicitly $R_k = R(\psi_k, \phi_k)$ with

$$R(\psi,\phi) = \begin{pmatrix} \cos^2(\psi) + \sin^2(\psi)\cos(\phi) & \sin(\psi)\cos(\psi)(1-\cos(\phi)) & \sin(\psi)\sin(\phi) \\ \sin(\psi)\cos(\psi)(1-\cos(\phi)) & \sin^2(\psi) + \cos^2(\psi)\cos(\phi) & -\cos(\psi)\sin(\phi) \\ -\sin(\psi)\sin(\phi) & \cos(\psi)\sin(\phi) & \cos(\phi) \end{pmatrix}.$$

From the probabilistic point of view, the angles $\phi_k$ are independent random variables uniformly distributed in $(0, 2\pi)$. The angles $\psi_k$ are independent random variables such that $\cos(\psi_k)$ are uniformly distributed in $(-1, 1)$ [5]. The fiber is modeled as the concatenation of $n$ segments and we are interested in the pdf tail of the final DGD $|\hat{\mathbf{r}}_n|$.

### 3.3. Estimations of outage probabilities

In Ref. [5] IS is used to accurately calculate outage probabilities due to PMD. The outage event can be represented as a set $A$ of particular realizations of the random process $\theta = (\theta_k)_{0\leqslant k\leqslant n-1} = (\psi_k, \phi_k)_{0\leqslant k\leqslant n-1}$, whose probability is denoted by $P_A$. The idea is to bias the distribution of $\theta$ so as to cause large DGD events to occur more frequently. Let us denote by $p$ the original distribution of $\theta$ (a direct product of uniform distributions as described above) and by $p^*$ a twisted distribution chosen by the user. We can carry out a set of $N$ MC simulations with the twisted distribution $p^*$ generating a set of independent $(\theta^{(i)})_{1\leqslant i\leqslant N}$. An estimator of the probability $P_A$ is

$$P_A^N = \frac{1}{N}\sum_{i=1}^{N} \mathbf{1}_A(\theta^{(i)}) \frac{p(\theta^{(i)})}{p^*(\theta^{(i)})}.$$

The key difficulty in applying IS is to properly choose $p^*$. The papers [5,21,22,11] present different twisted distributions and the physical explanations why such distributions are likely to produce large DGDs. As a result the authors obtain with $10^5$ MC simulations good approximations of the pdf tail even for probabilities of the order $10^{-12}$. The

main reported physical result is that the probability tail is significantly smaller than the Maxwellian tail predicted by the white noise model.

We now apply our IPS method and compare the results with those obtained by MC and IS. To get a reliable estimate of the outage probability of the event, it is necessary to generate realizations producing large DGDs. The main advantage of the IPS approach is that is proposes a non-intrusive and blink method that does not require any physical insight. Such a method could thus be generalized to more complicated situations. Here the physical quantity $X_k$ is the PMD vector $\hat{\mathbf{r}}_k$ at the output of the $k$th fiber section, it takes values in $\mathbb{R}^3$, the initial PMD vector is $\hat{\mathbf{r}}_0 = (0,0,0)^{\mathrm{T}}$, the random recursive equation (1) is described by Eq. (7), and the energy-like function is $V(\hat{\mathbf{r}}) = |\hat{\mathbf{r}}|$. We estimate the pdf $p(a)$ of $|\hat{\mathbf{r}}_n|$ by implementing the IPS with the weight function $G_k(\hat{\mathbf{r}}) = \exp[\alpha(|\hat{\mathbf{r}}_k| - |\hat{\mathbf{r}}_{k-1}|)]$ parameterized by $\alpha \geqslant 0$. In Fig. 1a we plot the estimation of the DGD pdf obtained by the IPS method. The fiber consists in the concatenation of $n = 15$ segments. The DGD per section is $\sigma = 0.5$. We use a set of $N = 2 \times 10^4$ interacting particles. This result can be compared with the one obtained in Ref. [5], which shows excellent agreement. The difference is that our procedure is fully adaptative and does not require any guess of the user. The ratio $p_2/p$ of the standard deviation of the estimator of the DGD pdf over the DGD pdf is plotted in Fig. 1b. This figure is actually used to determine the best estimator of the DGD pdf. Indeed the IPS and the corresponding estimator depends on the parameter $\alpha$. We have actually simulated three sets of particle systems, the first one being the usual MC method, the two other ones being IPSs with two different parameters $\alpha$. For each set of particle systems we have computed the empirical variances $p_2^2(a)$ by formula (5). For each value of $\tau$ we have detected which particle system gives rise to the smallest ratio $p_2/p(\tau)$. Then we report in Fig. 1b the value of this ratio, and in Fig. 1a we report the estimation $p(\tau)$ obtained with the corresponding particle system. This method allows us to get an accurate description of the DGD pdf, from the central part to the far tail. We can observe that the theoretical Maxwellian obtained with the white noise model accurately describes the DGD pdf for probabilities less than $10^{-6}$, but the pdf tail decays faster than the Maxwellian for smaller probability levels.

## 4. Pulse broadening in presence of random dispersion

One of the main limitations of high-bit rate transmission in optical fiber links is the chromatic dispersion. Two solutions have been proposed to compensate for the pulse broadening induced by dispersion. The first solution is the soliton transmission, where the dispersion is balanced by the Kerr non-linearity [20]. One of the main drawbacks is that four-wave mixing has been shown to be detrimental for wavelength-division multiplexing in a conventional soliton transmission line [23]. The second solution is a direct dispersion compensation for linear pulse propagation by the use of a periodic concatenation of pieces of fibers with opposite signs of dispersion [28]. However in any realistic optical network it will not be possible to compensate for all the dispersion in each element, so that there will remain some residual dispersion. Furthermore the amplitude of the signal is bounded from below to keep a reasonable signal-to-noise ratio, so that the non-linearity should also be taken into account. It was shown that the pulse propagation in such conditions was described by the non-linear Schrödinger (NLS) equation with a distance-varying dispersion coefficient [12]. As a result the concept of dispersion-managed (DM) soliton in dispersion compensated lines was proposed. It combines the advantages of the traditional fundamental soliton of the NLS equation, and the dispersion-managed non-return-to-zero signal transmission. Both computational and experimental investigations

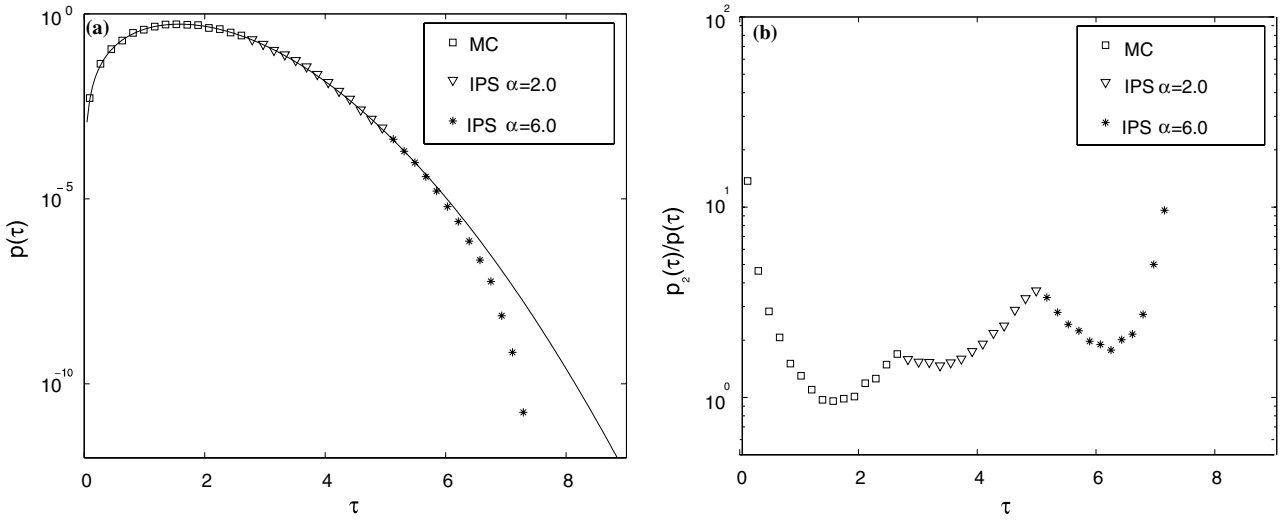


Fig. 1. (a) Segments of the DGD pdf obtained by the usual MC technique (squares) and by the IPS with $\alpha = 2.0$ (triangles) and $\alpha = 6.0$ (stars). The solid line stands for the Maxwellian distribution obtained in the white noise model. (b) Ratios $p_2/p$. In the MC case, the standard deviation is $p_2(\tau) = p(\tau)^{1/2}$. In the IPS cases, the standard deviations are estimated via formula (5).

have shown the existence and the stability of this new type of optical solitary wave (see [35] for a review). However it is well known that the NLS equation does not completely describe the pulse propagation in realistic fiber transmission links. In addition to the periodic dispersion management and non-linearity, random fluctuations of dispersion may occur [36]. Indeed measurements by a reflectometer yield the significance of dispersion randomness [25,18]. These terms have been shown to involve dramatic effects on the modulational instability of stationary waves because of a stochastic parametric resonance phenomenon [1]. In this section we shall analyze the stability of the DM soliton with respect to random fluctuations of the dispersion. For comparison we shall also analyze the stabilities of linear pulses and NLS solitons. As discussed in the previous section, the typical tolerance in telecommunication for the bit error rate is very low, which shows that the pdf tail is the interesting object. In a recent paper [27] importance sampling has been applied for the determination of the pdf tail of the pulse width driven by random dispersion. The authors develop very clever ways to deduce biasing rules for the application of IS strategy. Our goal in this section is to show that an IPS strategy can be easily implemented giving full access to the pdf tail of the pulse width in various regimes.

The propagation in a non-linear optical fiber is governed by the dimensionless NLS equation for the envelope of the electric field

$$\mathrm{i}u_z + \frac{d(z)}{2}u_{tt} + \gamma|u|^2u = 0, \tag{8}$$

where $d(z)$ is the GVD coefficient and $\gamma$ is the non-linear coefficient. We shall compute the pulse broadening in different regimes.

### 4.1. Pulse propagation in linear media

The pulse propagation in linear media is governed by the Schrödinger equation (8) with $\gamma = 0$. By going to the Fourier domain, we get an explicit expression of the rms pulse width. If the initial pulse has a Gaussian shape $u_0(t) = \exp[-t^2/(2T_0^2)]$ with rms width $T_{\mathrm{rms0}} = T_0/\sqrt{2}$, then

$$T_{\mathrm{rms}}^2(z) = T_{\mathrm{rms0}}^2\left[1 + c^2\frac{D(z)^2}{T_0^4}\right], \tag{9}$$

where $c = 1$ and $D(z) = \int_0^z d(\zeta)\,\mathrm{d}\zeta$ is the cumulative dispersion. If the initial pulse has a sech shape $u_0(t) = \mathrm{sech}(t/T_0)$ with rms width $T_{\mathrm{rms0}} = \pi T_0/\sqrt{12}$, then we still have (9) with $c = 2/\pi$. These closed-form formulae show that the pulse width can only increase whatever the initial profile. If the fiber is the concatenation of $n$ segments with length $l_c$ and GVD coefficients $d_j$ that obey independent Gaussian statistics with zero-mean and variance $\sigma^2$, then $D(z)$ obeys a Gaussian distribution with zero mean and variance $\Sigma^2 = \sigma^2 l_c n$. The statistical distribution of the pulse broadening can be readily estimated. The pdf of the ratio $R = T_{\mathrm{rms}}(z = nl_c)/T_{\mathrm{rms0}}$ is found to be

$$p(r) = \frac{\sqrt{2}r}{\sqrt{\pi r_1^2(r^2-1)}}\exp\left(-\frac{r^2-1}{2r_1^2}\right)\mathbf{1}_{[1,\infty)}(r), \tag{10}$$

where $r_1^2 = \langle(T_{\mathrm{rms}}/T_{\mathrm{rms0}})^2 - 1\rangle$ is equal to $4\Sigma^2/(\pi^2T_0^4)$ for the sech pulse and $r_1^2 = 36\Sigma^2/(\pi^4T_0^4)$ for the Gaussian pulse.

We have carried out numerical simulations to compare the results given by the MC and IPS methods with the theoretical pdf. The fiber consists in the concatenation of $n = 40$ segments with length $l_c = 0.1$ and GVD coefficients $d_j$ that obeys independent Gaussian statistics with zero-mean and variance $\sigma^2 = 0.1$. We use a set of $N = 2\times10^4$ interacting particles. Ten selection stages are performed at regularly spaced distances. The initial pulse is a sech pulse with $T_0 = 1$. In Fig. 2a we plot the segments of the pdf estimated by the MC method and by the IPS method. The choice between the two estimators of $p(r)$ is made by the determination of the minimum of the values $p_2/p(r)$ corresponding to each method (Fig. 2b). For low values of $r$, the MC estimator is the best estimator, but for high values of $r$ the IPS estimator has a much smaller variance.

Let us now address the full width at half maximum (FWHM), which is another way to characterize the pulse broadening. The relationship between the rms pulse width and the FWHM for a Gaussian pulse is $T_{\mathrm{FWHM}} = c_{\mathrm{shape}}T_{\mathrm{rms}}$ with $c_{\mathrm{shape}} = 2\sqrt{2\ln 2} \simeq 2.35$. The Gaussian shape is preserved by random dispersion, so the pdf of the FWHM can be deduced from the pdf of the rms width by a straightforward homotethy. As a consequence the pdf of the ratio $R = T_{\mathrm{FWHM}}(z)/T_{\mathrm{FWHM0}}$ is exactly the same as the pdf (10) of the ratio $R = T_{\mathrm{rms}}(z)/T_{\mathrm{rms0}}$. The relationship between the rms pulse width and the FWHM for a sech pulse is $T_{\mathrm{FWHM}} = c_{\mathrm{shape}}T_{\mathrm{rms}}$ with $c_{\mathrm{shape}} = 4\sqrt{3}\pi^{-1}\ln(1+\sqrt{2}) \simeq 1.94$. However, in this case, random dispersion does not preserve the sech shape, so it is not possible to deduce immediately the pdf of the FWHM from the pdf of the rms width. In Fig. 3a we plot the pdf of the FWHM for a sech pulse propagating in a random fiber of the same type as above. The solid line corresponds to the theoretical pdf that would be obtained if the output pulse was a sech pulse with the rms width (9). A noticeable departure with the numerical results can be observed, which is due to the fact that random dispersion imposes a shape deformation as described in Fig. 3b. This deformation induces a small modification of the rms pulse width, but a strong increase of the FWHM.

### 4.2. Soliton propagation in non-linear medium

We now address the propagation of a soliton in a randomly perturbed optical fiber. We take into account a non-linearity $\gamma = 1$, and assume that the GVD coefficient has mean 1: $d(z) = 1 + d_1(z)$. In absence of GVD fluctuations $d_1 \equiv 0$ the NLS equation supports soliton solution of the form $u_0(t) = T_0^{-1}\mathrm{sech}(t/T_0)$. We now study the stability of the NLS soliton versus GVD fluctuations. The

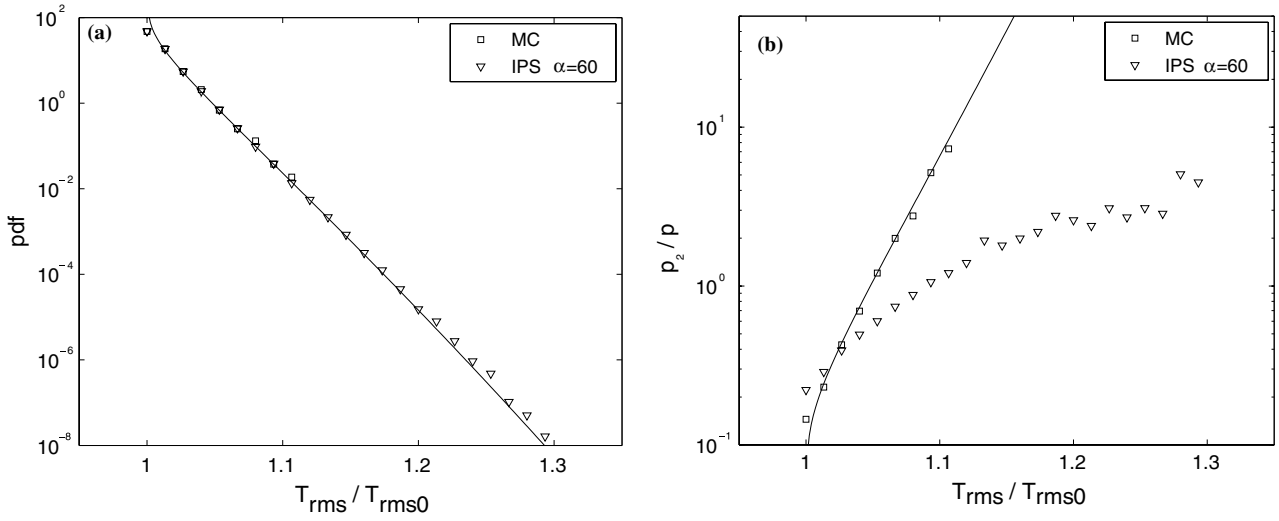


Fig. 2. (a) Pdf of the pulse broadening $R = T_{\mathrm{rms}}(z)/T_{\mathrm{rms0}}$ in the linear regime. The estimator is obtained by the usual MC technique (squares) and by the IPS with $\alpha = 60$ (triangles). The solid line stands for the theoretical distribution (10). (b) Ratio $p_2/p$ where $p_2$ is the estimated standard deviation. In the MC case, the standard deviation is $p_2(r) = p(r)^{1/2}$. In the IPS case, the standard deviation is estimated via formula (5).

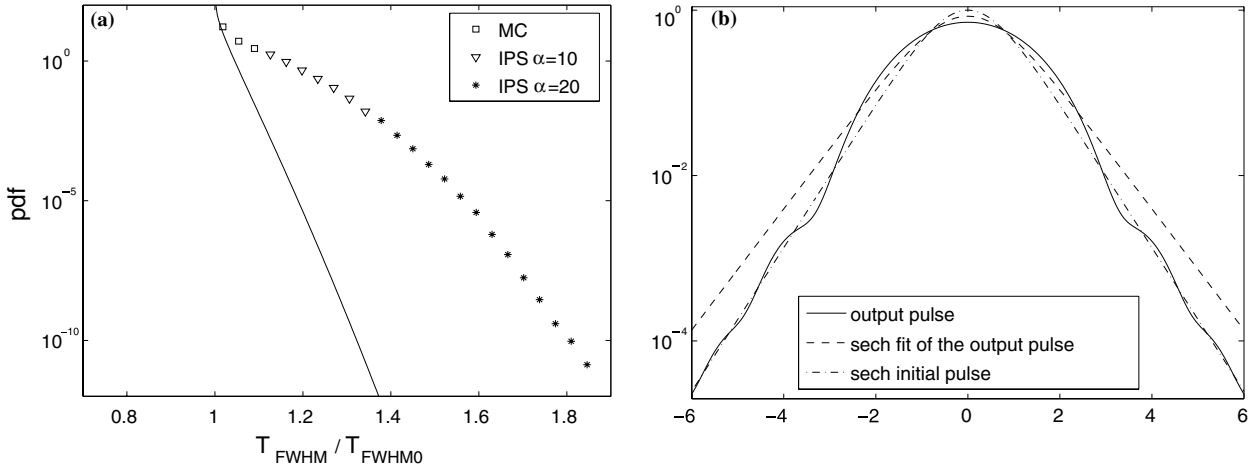


Fig. 3. (a) Pdf of the pulse broadening $T_{\mathrm{FWHM}}(z)/T_{\mathrm{FWHM0}}$ in the linear regime. The estimator is obtained by the usual MC technique (squares) and by the IPS with $\alpha = 10$ (triangles) and $\alpha = 20$ (stars). The solid line stands for the theoretical distribution (10). (b) Output pulse profile for one simulation (solid line). The sech fit of the output pulse profile is obviously wrong in the central part.

simulation scheme of the NLS equation is a split-step Fourier method. We use the model for the random fluctuations and the same numerical parameters as in the previous section. In Fig. 4, we plot the pdf of the pulse broadening $R = T_{\mathrm{rms}}(z)/T_{\mathrm{rms0}}$ estimated by the MC method and by the IPS methods with two different weight parameters $\alpha$. We compare with the pdf (10) corresponding to the linear propagation (in absence of GVD) which shows that the NLS soliton looks poorly stable. However, when we plot the pdf of the ratio $R = T_{\mathrm{FWHM}}(z)/T_{\mathrm{FWHM0}}$ in Fig. 5a, then we can see that the soliton looks more robust than the linear pulse. The opposite behaviors of the rms pulse width and the FWHM can be explained by considering the typical pulse profiles at the fiber output plotted in Figs. 3b and 5b.

(1) On the one hand, we can see in Fig. 5b that the sech soliton shape is very robust, because of the self-trapping induced by the non-linear potential. This stability can also be observed by comparing Figs. 4a and 5a since the pulse broadening measured in terms of the FWHM or in terms of the rms width are almost identical.

(2) On the other hand, random dispersion induces a significant shape deformation of a sech pulse in a random linear medium. As seen in Fig. 3b, the output pulse shape in the linear regime is not a sech anymore. This reshaping does not affect much the rms pulse width, but strongly increases the FWHM.

### 4.3. Dispersion-managed soliton in non-linear medium

The dispersion management (DM) technique for short pulse propagation in optical fibers has become a subject of great interest for telecommunication applications [34,33,12]. In dimensionless units the GVD coefficient $d$ is

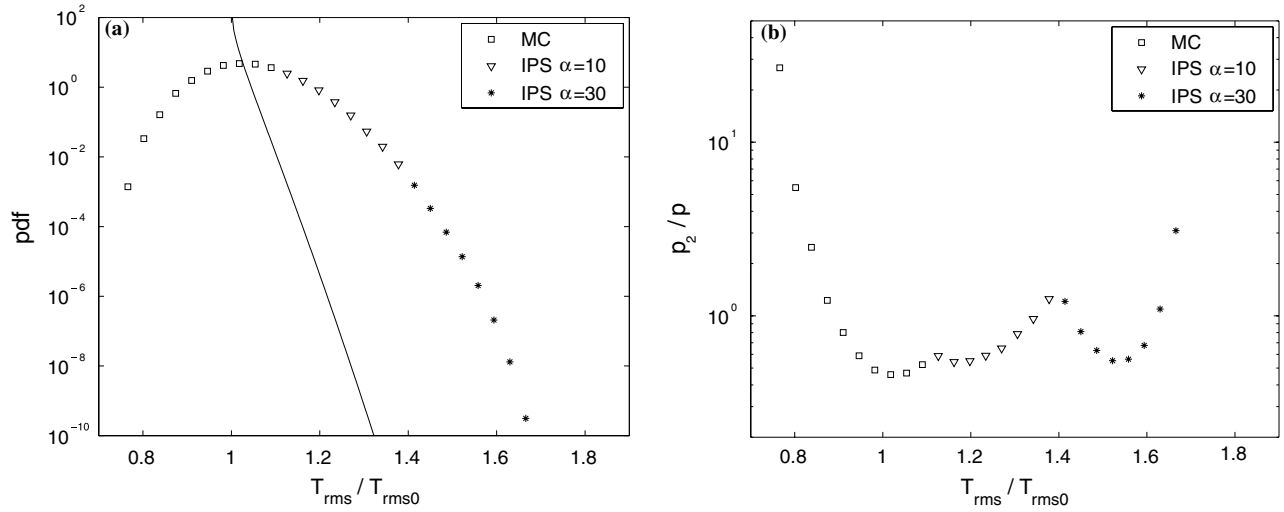


Fig. 4. (a) Pdf of the pulse broadening $T_{\mathrm{rms}}(z)/T_{\mathrm{rms0}}$ in the soliton regime. The pdf estimator is obtained by the usual MC technique (squares) and by the IPS with $\alpha = 10$ (triangles) and $\alpha = 30$ (stars). The solid line stands for the theoretical distribution obtained in the linear regime. (b) Ratio $p_2/p$ where $p_2$ is the estimated standard deviation.

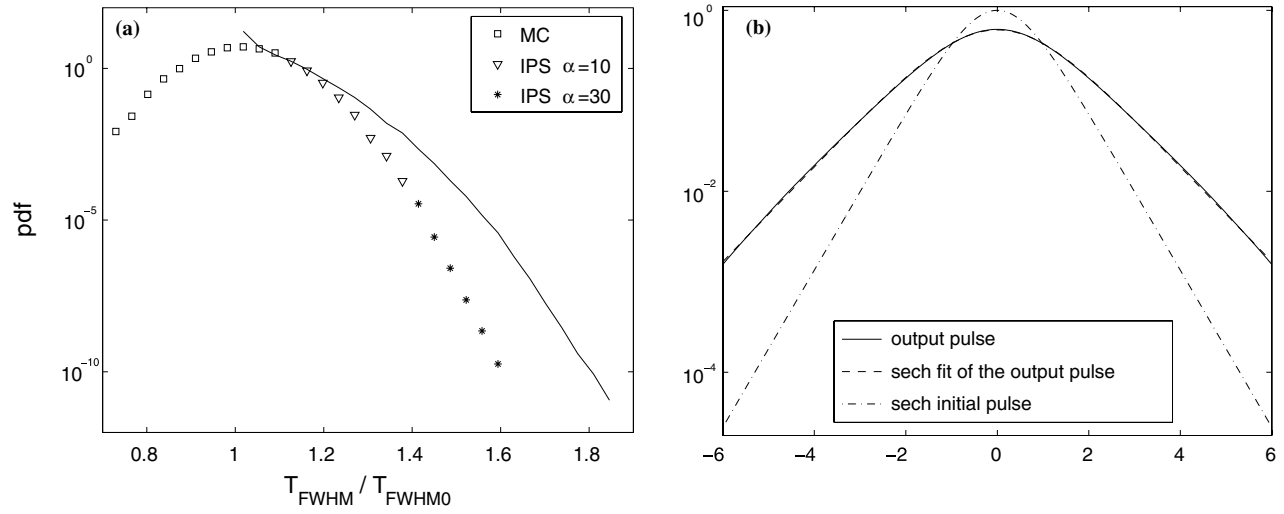


Fig. 5. (a) Pdf of the pulse broadening $T_{\mathrm{FWHM}}(z)/T_{\mathrm{FWHM0}}$ in the soliton regime. The estimator is obtained by the usual MC technique (squares) and by the IPS with $\alpha = 10$ (triangles) and $\alpha = 30$ (stars). The solid line stands for the pdf of the pulse broadening obtained in the linear case with zero-mean GVD (Fig. 3a). (b) Output pulse profile for one simulation (solid line). The sech fit of the output pulse profile is obviously very accurate.

of the form $d(z) = d_0(z) + d_m + d_1(z)$ where $d_0$ represents the zero-mean periodic variation with period $l_{\mathrm{map}} = l_+ + l_-$

$$d_0(z) = \begin{cases} d_+ & \text{if } z \in [0, l_+/2), \\ d_- & \text{if } z \in [l_+/2, l_{\mathrm{map}} - l_+/2), \\ d_+ & \text{if } z \in [l_{\mathrm{map}} - l_+/2, l_{\mathrm{map}}). \end{cases}$$

The so-called dispersion management (DM) strength is $D_L := d_+ l_+ = -d_- l_-$. $d_m$ is the residual average dispersion of the dispersion-management map. $d_1$ models the random GVD fluctuations.

A DM soliton in an unperturbed fiber can be determined using the numerical routine prescribed in Ref. [28]. We consider two dispersion maps with the parameters $d_m = 1$, $l_+ = l_- = 0.1$, $D_L = 10$ and $D_L = 5$. The map with $D_L = 10$ supports a DM soliton whose rms pulse width at the middle of each span is $T_{\mathrm{rms0}} \simeq 1.68$, and whose energy is $\int |u|^2 \,\mathrm{d}t \simeq 1.77$. The map with $D_L = 5$ supports a DM soliton whose rms pulse width is also $T_{\mathrm{rms0}} \simeq 1.68$, and whose energy is $\int |u|^2 \,\mathrm{d}t \simeq 1.30$. The power enhancement arising from increased map strength is noticeable. If we consider in more detail the power profiles of the DM soliton, then we find that the energy bearing parts of the profiles are Gaussian-like, but the tails are not Gaussian at all. We now examine the effects of random GVD fluctuations. More exactly we consider a random process $d_1$ which is stepwise constant over elementary intervals with length $l_c = 0.1$ and take values $m_j$ over the $j$th interval. The $m_j$'s are assumed to be independent Gaussian random variables with variance $\sigma^2 = 0.5$. Note that the GVD vari-

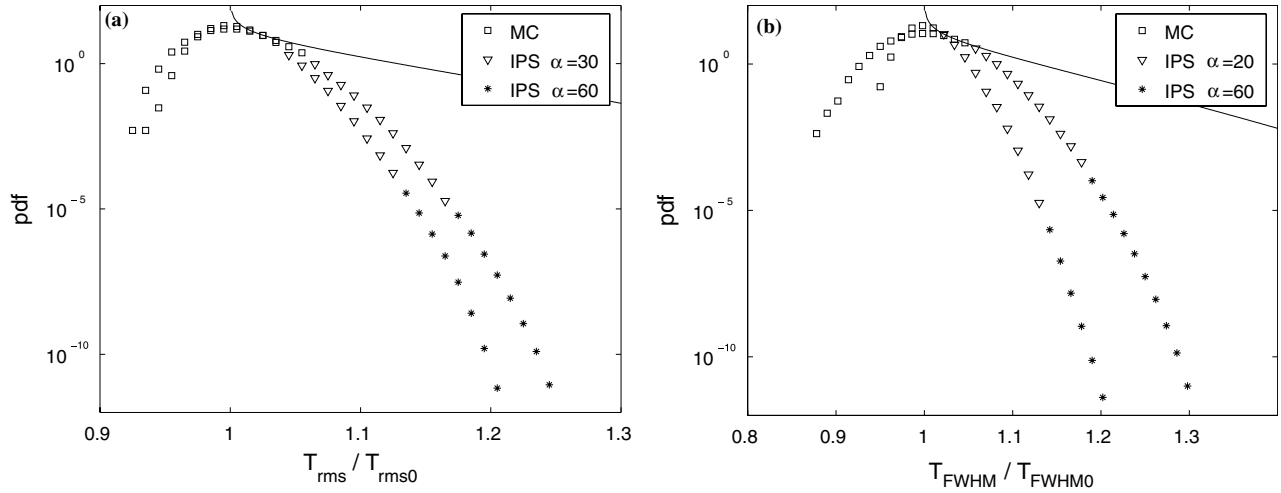


Fig. 6. (a) Pdfs of the pulse broadening $T_{\mathrm{rms}}(z)/T_{\mathrm{rms0}}$ for two DM solitons with $D_L = 5$ and $D_L = 10$ (from broadest to narrowest). We compare the results obtained by the usual MC technique (squares) and by the IPS with different values for $\alpha$ (triangles and stars). The solid line stands for the theoretical distribution obtained in the linear regime with a Gaussian pulse. (b) Pdfs of the pulse broadening $T_{\mathrm{FWHM}}(z)/T_{\mathrm{FWHM0}}$ for the same pulses.

ance is five times larger than in the previous sections, because the DM soliton turns out to be very robust and large GVD fluctuations are necessary to get a non-negligible pulse broadening. The DM solitons are launched in the middle of the first span. For each simulation we record the rms pulse width $T_{\mathrm{rms}}(z)$ at the middle of the last span, where $z = 4$ corresponds to the concatenation of 40 maps. In Fig. 6 we plot the pdf of the ratio $R = T_{\mathrm{rms}}(z)/T_{\mathrm{rms0}}$. We compare it with the pdf (10) of the pulse broadening of a Gaussian pulse in the linear propagation regime. We can observe that the DM soliton is much more robust than the equivalent Gaussian pulse in a linear medium. We also note that the robustness increases with the map strength. The same behaviors are observed when plotting the pdf of the ratio $R = T_{\mathrm{FWHM}}(z)/T_{\mathrm{FWHM0}}$, which is another evidence of the shape robustness of the DM soliton. These results are in agreement with the theoretical predictions using the variational approach [14] and with recent numerical simulations using IS strategy [27].

## 5. Conclusion

We have shown that the IPS strategy is efficient for estimating rare event probabilities on two examples: occurrence of large DGD driven by PMD, and occurrence of critical pulse broadening driven by random dispersion. In the first problem, we have shown that the DGD pdf tail is not Maxwellian as predicted by the white noise theory. In the second problem, we have compared the pulse broadening of linear pulses, solitons, and DM solitons. The most robust pulse if the DM soliton, as predicted by the variational approach. The comparison of the NLS soliton and linear pulses is more delicate, and our conclusions should help interpreting recent results [27]. When we compare the rms pulse widths, we get the conclusion that the NLS soliton is less stable than the equivalent sech pulse in the linear regime. However, when we compare the FWHM of the pulses, the NLS soliton appears to be robust because it retains its sech shape, while in the linear regime the sech shape is very rapidly modified and the reshaping induces a significant increase of the FWHM.

The IPS method could be easily implemented in other configurations modeled by random dynamical systems. In contrast to IS and other biasing MC methods, the IPS method does not require from the user to guess and implement a biasing strategy to estimate the pdf tail of an output random variable. Instead, selection steps are implemented where the performances of the particles are evaluated and compared. The central brain of the IPS allows the good particles to have many children in order to probe further the state space, while it kills those particles that are not efficient enough. As a result, the first advantage of the IPS method is that the user has nothing to do, but to increase (resp. decrease) the parameter $\alpha$ that controls the selection pressure to probe the far (resp. near) tail of the pdf. The second advantage is that the IPS strategy can be implemented in a non-intrusive way, without modifying a pre-existing code, because only the true, i.e. unbiased, system is simulated.

## References

[1] F.Kh. Abdullaev, S.A. Darmanyan, A. Kobyakov, F. Lederer, Phys. Lett. A 220 (1996) 213.
[2] B.A. Berg, Fields Inst. Commun. 26 (2000) 1.
[3] G. Biondini, W.L. Kath, Photon. Technol. Lett. 17 (2005) 1866.
[4] G. Biondini, W.L. Kath, C.R. Menyuk, Proc. OFC 2001 ThA5 (2001) 1.
[5] G. Biondini, W.L. Kath, C.R. Menyuk, Photon. Technol. Lett. 14 (2002) 310.
[6] G. Biondini, W.L. Kath, C.R. Menyuk, J. Lightwave Technol. 9 (2004) 1201.
[7] H. Bülow, Proc. ECOC 1999 WE1 (1999) 74.
[8] P. Del Moral, Feynman–Kac Formulae, Genealogical and Interacting Particle Systems with Applications, Springer, New York, 2004.
[9] P. Del Moral, J. Garnier, Ann. Appl. Probab. 15 (2005) 2496.

[10] A. Doucet, N. de Freitas, N. Gordon, Sequential Monte Carlo Methods in PracticeStatistics for Engineering and Information Science, Springer, New York, 2001.
[11] S.L. Fogal, G. Biondini, W.L. Kath, Photon. Technol. Lett. 14 (2002) 1273.
[12] I. Gabitov, S.K. Turitsyn, Opt. Lett. 21 (1996) 327.
[13] A. Galtarossa, G. Gianello, C.G. Someda, M. Schiano, J. Lightwave Technol. 14 (1996) 42.
[14] J. Garnier, Opt. Commun. 206 (2002) 411.
[15] J. Garnier, J. Fatome, G. Le Meur, J. Opt. Soc. Am. B 19 (2002) 1968.
[16] N. Gisin, J.P. Pellaux, J.P. Von der Weid, J. Lightwave Technol. 9 (1991) 821.
[17] J.P. Gordon, H. Kogelnik, Proc. Nat. Acad. Sci. 97 (2000) 4541.
[18] J. Grip, L.F. Mollenauer, Opt. Lett. 23 (1998) 1603.
[19] T.E. Harris, H. Kahn, Natl. Bur. Stand. Appl. Math. Ser. 12 (1951) 27.
[20] A. Hasegawa, F. Tappert, Appl. Phys. Lett. 23 (1973) 142.
[21] I.T. Lima Jr., G. Biondini, B.S. Marks, W.L. Kath, C.R. Menyuk, Photon. Technol. Lett. 14 (2002) 627.
[22] A.O. Lima, I.T. Lima, C.R. Menyuk, J. Lightwave Technol. 23 (2005) 3781.
[23] P.V. Mamyshev, L.F. Mollenauer, Opt. Lett. 21 (1996) 396.
[24] D. Marcuse, C.R. Menyuk, P.K.A. Wai, J. Lightwave Technol. 15 (1997) 1735.
[25] L.F. Mollenauer, P.V. Mamyshev, M.J. Neubelt, Opt. Lett. 21 (1996) 1724.
[26] R.O. Moore, G. Biondini, W.L. Kath, Opt. Lett. 28 (2003) 105.
[27] R.O. Moore, T. Schäfer, C.K.R.T. Jones, Opt. Commun. 256 (2005) 439.
[28] J.H.B. Nijhof, N.J. Doran, W. Forysiak, F.M. Knox, Electron. Lett. 33 (1997) 1726.
[29] C.D. Poole, R.E. Wagner, Electron. Lett. 22 (1986) 1029.
[30] S.C. Rashleigh, J. Lightwave Technol. 1 (1983) 312.
[31] M.N. Rosenbluth, A.W. Rosenbluth, J. Chem. Phys. 23 (1955) 356.
[32] R.Y. Rubinstein, Simulation and the Monte Carlo Method, Wiley, New York, 1981.
[33] N.J. Smith, F.M. Knox, N.J. Doran, K.J. Blow, I. Bennion, Electron. Lett. 32 (1996) 54.
[34] M. Suzuki, I. Morita, N. Edagawa, S. Yamamoto, H. Taga, S. Akiba, Electron. Lett. 31 (1995) 2027.
[35] S.K. Turitsyn, T. Schäfer, K.H. Spatschek, V.K. Mezentzev, Opt. Commun. 163 (1999) 122.
[36] S. Wabnitz, Y. Kodama, A.B. Aceves, Opt. Fiber Technol. 1 (1995) 187.
[37] P.K.A. Wai, C.R. Menyuk, J. Lightwave Technol. 14 (1996) 148.